Applied Catalysis B: Environmental 121–122 (2012) 223–229

Contents lists available at SciVerse ScienceDirect

Applied Catalysis B: Environmental

journal homepage: www.elsevier.com/locate/apcatb

# $CeO_2/H_2O_2$ system catalytic oxidation mechanism study via a kinetics investigation to the degradation of acid orange 7

Feng Chen*, Xingxing Shen, Yongchuan Wang, Jinlong Zhang

*Key Laboratory for Advanced Materials and Institute of Fine Chemicals, East China University of Science and Technology, 130 Meilong Road, Shanghai 200237, PR China*

ARTICLE INFO

*Article history:*
Received 29 November 2011
Received in revised form 12 March 2012
Accepted 11 April 2012
Available online 17 April 2012

*Keywords:*
Ceria
Hydrogen peroxide
Peroxide species
Adsorption
Kinetics
$Ce^{3+}$

ABSTRACT

Nano ceria with cubic lattice was prepared and characterized by X-ray diffraction (XRD) and transmission electron microscopy (TEM) techniques. Degradation kinetics of acid orange 7 (AO7) was investigated to understand the catalytic oxidation mechanism of the $CeO_2$ with $H_2O_2$. The degradation of AO7 relies significantly on its adsorption on the surface of $CeO_2$ with an apparent order of 2.40. Increasing the concentration of $H_2O_2$ increases the degradation reaction rate constant of AO7 in a positive linear relationship at the initial stage, but later hinders further degradation of AO7 due to over-complexation of $Ce^{3+}$ with $H_2O_2$. The catalytic kinetics of $CeO_2$ in pre-adsorbed mode (AO7 pre-adsorbed on $CeO_2$ before the addition of $H_2O_2$) and pre-mixed mode ($CeO_2$ pre-mixed with $H_2O_2$ before the addition of AO7) is quite different. The pre-mixed mode is unfavorable for AO7 degradation, as almost all of surface $Ce^{3+}$ are pre-oxidized into surface peroxide species with $H_2O_2$ and hence reduces adsorption of AO7 as well as the activation of AO7 degradation. Reversely, the reactivity of $CeO_2$ can slowly be recovered by adsorption of AO7, which competitively adsorbs on the $CeO_2$ and gradually initiates the release of the surface $Ce^{3+}$ by consuming the surface peroxide species. The AO7 degradation kinetics investigation in this work verifies that the degradation of organics in $CeO_2/H_2O_2$ system is adsorption-triggered and the $Ce^{3+}$ in reduced state is essential for activating the catalytic oxidation activity of surface peroxide species. EPR studies show that the surface peroxide species oxidizes the organics via hydroxyl adduct route.

© 2012 Elsevier B.V. All rights reserved.

## 1. Introduction

Cerium oxide is one of the most reactive rare earth metal oxides and has been extensively used in numerous fields, such as catalytic converters for automobile exhaust systems (TWC) [1], water-gas shift reactions (WGS) [2,3], oxygen storage capacitors (OSC) [4,5], UV blockers [6], and electrolytes for solid oxide fuel cells (SOFC) [7–9]. In particular, there is great interest in redox catalytic applications for cerium oxide due to its rich oxygen vacancies and low redox potential between $Ce^{3+}$ and $Ce^{4+}$ [10–14].

The catalytic activity of $CeO_2$ relies closely on the redox cycle of $Ce^{4+}/Ce^{3+}$. In recent years, nanoceria has also been tested in both animal and cell culture models to determine its role against oxidative stress [14–20]. The $Ce^{3+}$ surrounding the oxygen vacancy catalyzes the dismutation of oxidative stress such as superoxide radical, which seems to be inhibited by the high concentrations (100 mM to 1.0 M) of hydrogen peroxide [16], as $Ce^{3+}$ would be occupied and oxidized to $Ce^{4+}$ by $H_2O_2$ [18]. In environmental remediation studies, along with the catalytic wet oxidation (CWO) with nano-$CeO_2$ and $CeO_2$-based materials [21,22], Fenton-like reaction catalyzed by cerium salt in the presence of $H_2O_2$ has also been reported for the removal of organics from polluted water [17,23]. Specifically, it was proposed that the reaction of cerium and $H_2O_2$ underwent the cycle of $Ce^{4+}/Ce^{3+}$ with the generation of superoxide and hydroxyl radical, which was later referred to understand the reaction of $CeO_2$ with $H_2O_2$ [17]. However, our previous studies [24,25] show that the peroxide-like species ($O_2^{2-}$) formed on the surface of $CeO_2$ in the $CeO_2/H_2O_2$ system are relatively chemically stable in the absence of the organic contaminants and can only degrade substances adsorbed on the surface of $CeO_2$ via an intermolecular rearrangement.

In our proposed mechanism [24,25], the interfacial peroxide-like species is generated via the interaction of $H_2O_2$ with $Ce^{3+}$; its reactivity to the adsorbed organics relies on the neighboring $Ce^{3+}$ for activation, and hence can be blocked with high concentrations of hydrogen peroxide [16]. However, to what extent does the surface $Ce^{3+}$ determine the reactivity of $CeO_2/H_2O_2$ system still lacks a requisitely experimental observation, which is of importance to verify the reliability of our proposed mechanism [25].

Herein, a kinetic investigation on the degradation of organics in the aqueous $CeO_2/H_2O_2$ system is carried out. A typical azo-dye, acid orange 7 (AO7), was chosen as the model target to examine

* Corresponding author. Tel.: +86 21 6425 2062; fax: +86 21 6425 2062.
*E-mail addresses:* fengchen@ecust.edu.cn (F. Chen), shenxingxing87@163.com (X. Shen), fjaxwyc@sina.com (Y. Wang), jlzhang@ecust.edu.cn (J. Zhang).

0926-3373/$ – see front matter © 2012 Elsevier B.V. All rights reserved.
http://dx.doi.org/10.1016/j.apcatb.2012.04.014

the adsorption and degradation of organics in a normal or an inhibited $CeO_2/H_2O_2$ system. DMPO spin trapping EPR spectroscopy measurements were also done to follow the level of the reactive oxidation species formed in the $CeO_2/H_2O_2$ system.

## 2. Experimental

### 2.1. Materials

$Ce(NO_3)_3{\cdot}6H_2O$ and $H_2O_2$ (30%) were supplied by Shanghai Sinopharm Chemical Reagent. AO7 dye was obtained from Acros. The radical spin trap, 5,5-dimethyl-1-pyrroline N-oxide (DMPO) (purity > 97%), was purchased from Tokyo Chemical Industry. All of the chemicals were of analytic grade and were used without further purification. Doubly distilled water was used throughout this study.

### 2.2. $CeO_2$ preparation

$CeO_2$ was prepared with a precipitation method [26]. 4.34 g $Ce(NO_3)_3{\cdot}6H_2O$ was dissolved in 100 mL of distilled water to form a transparent solution (0.1 M). Then 4.0 mL $NH_3{\cdot}H_2O$ (28 wt%) was quickly added into the solution under vigorous stirring to form a yellowish suspension. The suspension was stirred continuously for 2 h at 40 °C followed by 12 h aging at 40 °C. The as-formed purple precipitate was collected by centrifugation and washed 3 times with water and dried at 60 °C for 12 h. Finally, the catalysts were obtained after grinding and calcination under ambient air at 500 °C for 4 h (ramp up: 2 °C/min).

### 2.3. Catalyst characterization

The powder X-ray diffraction (XRD) analysis of the prepared catalyst was carried out at room temperature with a Rigaku D/max 2550 VB/PC apparatus using Cu Ka radiation ($\lambda = 0.15406$ nm) and a graphite monochromator, operated at 40 kV and 30 mA. Diffraction patterns were recorded in the angular range of 10–80°. The BET specific surface area ($S_{BET}$) was determined by nitrogen adsorption at 77.3 K (Micromeritics ASAP 2020). Samples were degassed at 473 K for 5 h prior to the measurement. The morphology of the samples was observed by high-resolution transmission electron microscopy (HRTEM, JEOL JEM 2000-EX) with an electron beam accelerating voltage of 200 kV. Electron Paramagnetic Resonance (EPR) measurements for the catalyst powders were recorded at room temperature on a Bruker EMX-8/2.7 by accumulating three scans with the microwave frequency of 9.85 GHz and power of 6.35 mW. Both untreated and $H_2O_2$ pretreated catalysts were placed into a glass capillary in pasty form. DMPO trapping measurements were taken at room temperature by adding DMPO (50 mM) into the reaction suspension and recorded by one scan.

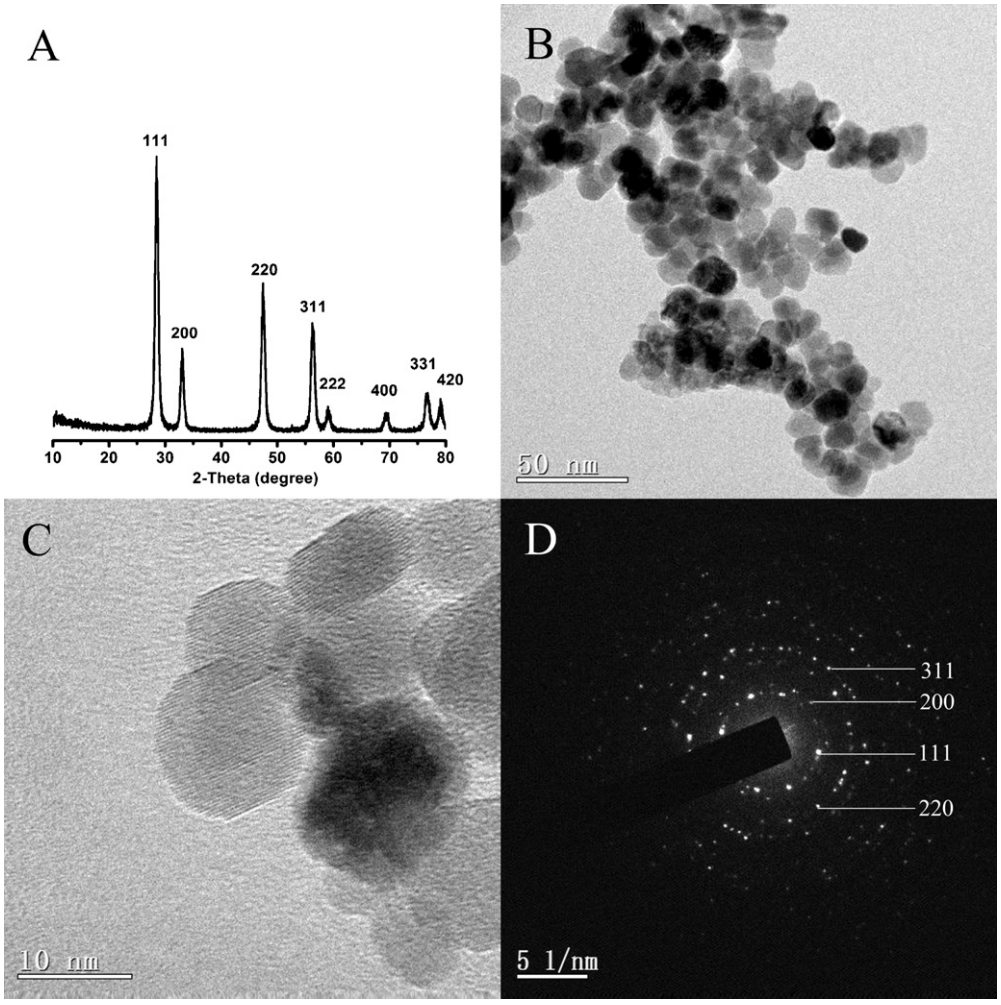


**Fig. 1.** (A) XRD pattern, (B, C) TEM images, and (D) SAED pattern of the as-prepared $CeO_2$ sample.

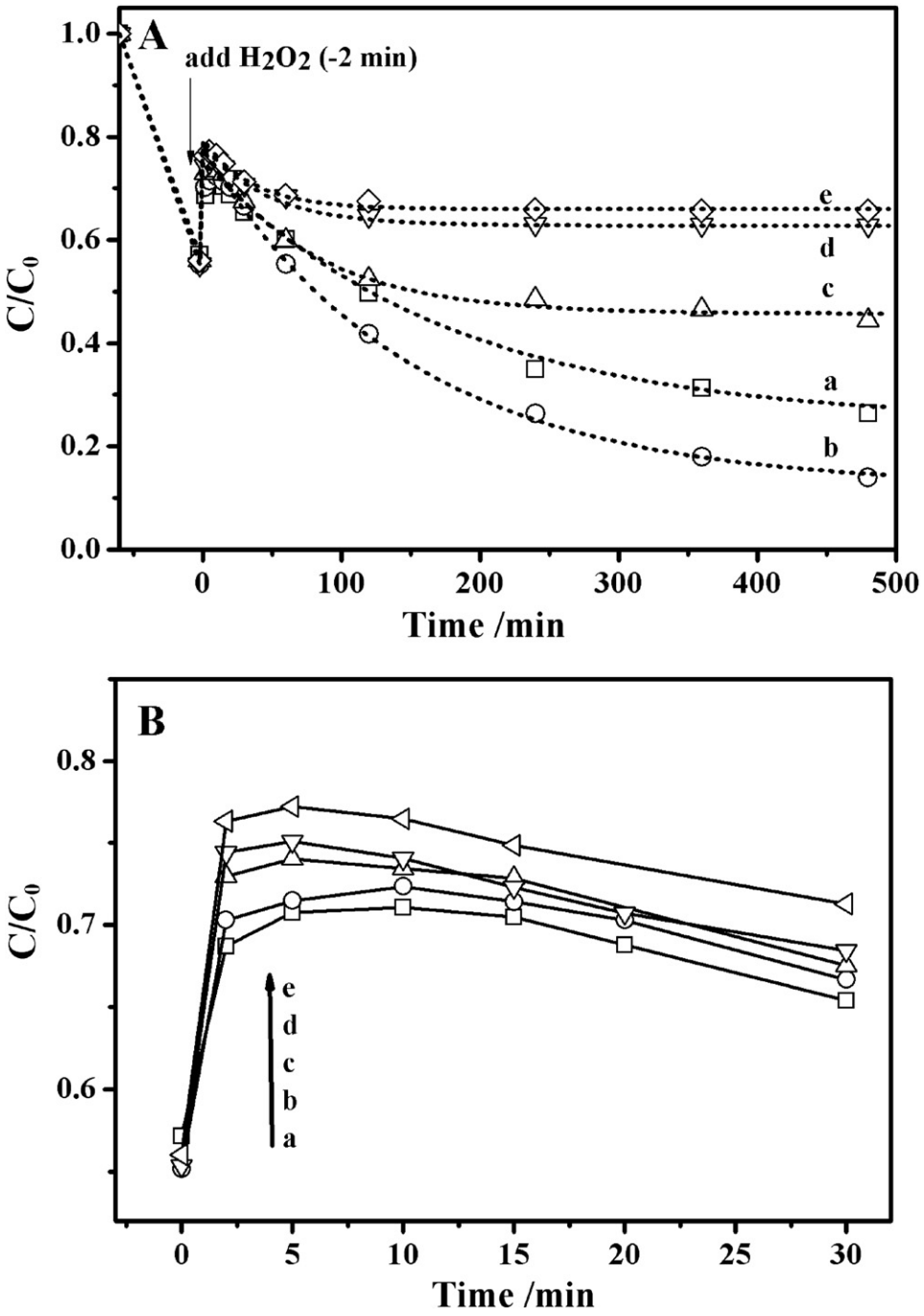


**Fig. 2.** Adsorption and degradation of AO7 in $CeO_2/H_2O_2$ system with (a) 5 mM, (b) 10 mM, (c) 20 mM, (d) 40 mM, and (e) 80 mM of $H_2O_2$ in a time range of (A) 500 min, and (B) 30 min. Plot: experimental data; dot line: fitting data. [$CeO_2$] = 0.5 g/L, [AO7] = 35 mg/L.

### 2.4. Measurements of catalytic activity

The catalytic activity was evaluated by measuring the decompositions of the AO7 (35 mg/L) aqueous solution with the addition of $H_2O_2$ in dark. In a typical degradation experiment, the catalyst powders (0.05 g) were added into a quartz tube containing 100 mL AO7 solution. The suspensions were stirred in the dark for 1.0 h to ensure the establishment of an adsorption–desorption equilibrium. Then $H_2O_2$ solution was added to reach a concentration of 10 mM. At the given time intervals, samples were taken from the mixture and immediately filtered with a micropore membrane (0.22 μm). The residual AO7 levels in the filtrates were then analyzed by recording variations of the absorbance at 484 nm with a UV–vis spectrophotometer (SHIMADZU UV-2450). All the reactions were carried out in the dark.

## 3. Results and discussion

### 3.1. Characterizations of the $CeO_2$ catalyst

The XRD pattern of the as-prepared $CeO_2$ catalyst is shown in Fig. 1. $CeO_2$ catalyst displays a typical XRD pattern of cubic $CeO_2$ (fluorite structure, JCPDS 34-0349). The average grain size of the $CeO_2$ estimated by Scherrer equation from its XRD pattern is ca.

13.1 nm ($D_{111}$). TEM images in Fig. 1B and C present $CeO_2$ nanocrystallites with grain sizes of ca. $12 \pm 2$ nm, which is consistent with the XRD results. The SAED pattern in Fig. 1D also confirms that $CeO_2$ has fluorite structure of high crystallinity. The specific surface area of the as-prepared $CeO_2$ catalyst is 59.6 $m^2/g$.

### 3.2. Degradation kinetics of AO7 with $CeO_2/H_2O_2$ system

$H_2O_2$ prefers to complex with cerium ion on the surface of $CeO_2$ to form surface peroxide species, which then carries out an intermolecular rearrangement with the neighboring adsorbed organic compounds to achieve the oxidation of organics [25,26]. In our previous work, some organics such as AO7, salicylic acid and sodium dodecylbenzenesulfonate were found to be decomposed smoothly with the $CeO_2/H_2O_2$ system [26].

Fig. 2 presents the degradation of azo-dye AO7 with as-prepared $CeO_2$ catalyst in the presence of various concentrations of $H_2O_2$ in the dark. AO7 adsorbs greatly on the surface of $CeO_2$. Ca. $44.0 \pm 1.0\%$ of the concentration decrease of AO7 can be observed in 1 h before the addition of $H_2O_2$. The addition of $H_2O_2$ induces a quick desorption of AO7 via a competitive adsorption on the surface of $CeO_2$; however, the level of desorption cannot be well quantified due to the synchronously catalytic decomposition of AO7. Strangely, $H_2O_2$ concentration of 10 mM exhibits the greatest degradation of AO7, while that of 80 mM presents the minimum degradation of AO7 in a time scale of 8 h. On the other hand, some special information can be obtained from the concentration variations of AO7 in the initial stage (after the addition of $H_2O_2$). Increasing the $H_2O_2$ concentration leads to a greater and quicker desorption of AO7 and a significant decrease in initial AO7 concentration (the first 30 min as shown in Fig. 2B). The degradation rate of AO7 increases with the increase in $H_2O_2$ concentration at the initial stage, which however decreases with time. Higher concentration of $H_2O_2$ induces more remarkable slowing down of the AO7 concentration decrement as shown in Fig. 2A. The AO7 concentration decrement can be well-fitted in apparent first order kinetics as shown in Fig. 2A (dot lines). The AO7 degradation rate constant then can be quantified from the life-time of these first-order exponential decay lines according to the Eq. (1).

$$k = \frac{1}{\tau} \tag{1}$$

One should note that the AO7 degradation rate constant $k$ here is just related to the quick degradation of AO7 in a time range of 480 min. Slow degradation of AO7 (which seems possible as shown in Fig. 4b), if exists, cannot be reflected here. Fig. 3 shows the

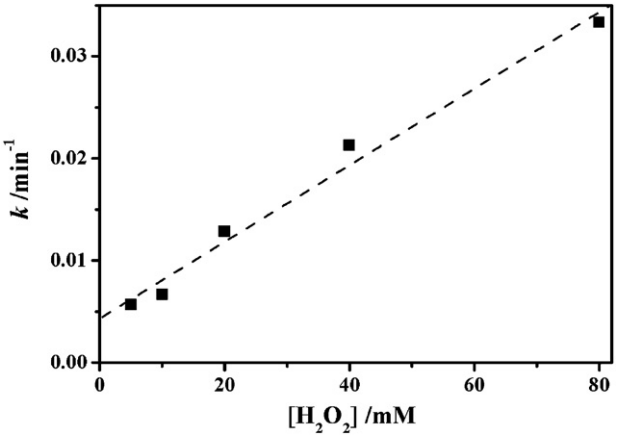


**Fig. 3.** The degradation rate constant vs the initial concentration of $H_2O_2$.

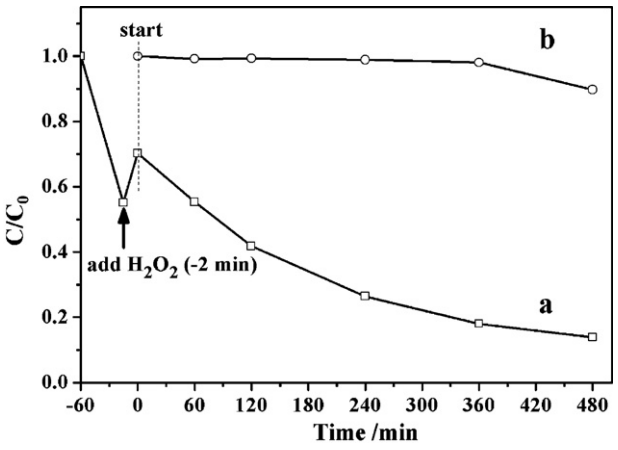


**Fig. 4.** Adsorption and degradation of AO7 in $CeO_2/H_2O_2$ system with different operation processes: (a) pre-adsorbed mode and (b) pre-mixed mode. [$CeO_2$] = 0.5 g/L, [AO7] = 35 mg/L.

relationship of the AO7 degradation rate constant ($k$) with the initial $H_2O_2$ concentration, which gives a linear positive correlation.

It is worth noting that the degradation rate of AO7 in the presence of 80 mM $H_2O_2$ after 120 min is tens of times slower than in the initial time in Fig. 2A. Such an apparent kinetics change should not be just due to the concentration quenching (trapping) effect of $H_2O_2$. Fig. 4 shows the degradation of AO7 with different operation processes—catalyst ($CeO_2$) is pre-adsorbed with AO7 before the addition of $H_2O_2$ as normal (Fig. 4a, pre-adsorbed mode) and/or pre-mixed with $H_2O_2$ before the addition of AO7 (Fig. 4b, pre-mixed mode). As shown in Fig. 4, the difference in the operation process resulted in a great difference in AO7 degradation kinetics. Only 1.9% and 11.3% of the AO7 were degraded in the pre-mixed mode, while ca. 52.3% and 56.4% of the AO7 were decomposed in the pre-adsorbed mode in 360 min and 480 min, respectively.

Surely, the charging sequence is essential for the catalytic oxidation reactivity of $CeO_2$. Another interesting issue should be mentioned in Fig. 4 is that the concentration decrease of AO7 is hardly observed even after 6 h of reaction for the pre-mixed mode, although reaction time is long enough for achieving an adsorption/desorption equilibrium for AO7 and $H_2O_2$ on the surface of $CeO_2$. In our previous work, we found that the catalytic oxidation of organics in $CeO_2/H_2O_2$ system is an interfacial reaction and the adsorption of organics on $CeO_2$ nano-particles is a prerequisite for its degradation [25]. A logical hypothesis is thus in the pre-mixed mode, $H_2O_2$ inhibits the degradation of AO7 by blocking its adsorption on the surface of $CeO_2$. The adsorption-blocking hypothesis can also justify the abnormal phenomena observed in Fig. 2A in which the degradation of AO7 is relatively quicker in the initial time but then significantly slows down and even stops (see that with 40 mM and 80 mM $H_2O_2$) with higher concentration of $H_2O_2$. On the other hand, the oxidation of $Ce^{3+}$ by $H_2O_2$ in the absence of AO7 (Fig. 4b) should also be seriously considered, which seems to be significantly intercepted by the adsorbed AO7 (Fig. 4a). The catalytic oxidation performance of $CeO_2$ towards the Reactive oxygen species (ROS) has been suggested to be related to the $Ce^{3+}$ sites on the surface of $CeO_2$, e.g., the superoxide radical dismutation with $CeO_2$ was found to be inhibited by high concentrations of $H_2O_2$ owing to the oxidation of $Ce^{3+}$ to $Ce^{4+}$ by $H_2O_2$ [16].

The interfacial reaction of AO7 in $CeO_2/H_2O_2$ system can be described as an intermolecular interaction of surface peroxide species with adsorbed AO7; hence, the apparent degradation rate of AO7 seems to have a positive correlation to the amounts of adsorbed $H_2O_2$ and AO7 (Eq. (2)).

$$r = k[O_{ads}][L_{ads}] \tag{2}$$

Here $O_{ads}$ refers to the surface peroxide species resulting from the surface complexation of $H_2O_2$ with cerium ion, $L_{ads}$ is the adsorbed AO7, while $k$ is the theoretical reaction rate constant. However, some literatures [1,3] reported that the catalytic oxidation process (with $O_2$) prefers to take place near the oxygen vacancies (i.e. $Ce^{3+}$) in the WGS process, while our previous work [24,25] showed that the primary reaction between the surface peroxide species and the adsorbed organics depends greatly on the neighboring $Ce^{3+}$ for activation. Considering that the amount of $L_{ads}$ may alter the concentration of $Ce^{3+}$ on the surface of $CeO_2$ via competitive adsorption and/or $O_{ads}$ consumption, the theoretical reaction rate constant, $k$, should also be related to the amounts of $O_{ads}$ and $L_{ads}$. Therefore, the apparent degradation rate of AO7 can be further calculated as follows (Eq. (3)),

$$r = k'[O_{ads}][L_{ads}]^n \quad (3)$$

$k'$ is reaction rate constant after deducting the factors from $[L_{ads}]$ and thus relatively fixed, while $n$ is the apparent orders of reaction towards $L_{ads}$. Therefore,

$$\frac{r}{r_0} = \frac{[O_{ads}][L_{ads}]^n}{[O_{ads}]_0[L_{ads}]_0^n} \quad (4)$$

Here $r_0$, $[O_{ads}]_0$ and $[L_{ads}]_0$ are corresponding values obtained in one randomly designated condition. Since $H_2O_2$ has very strong chemical interaction with $CeO_2$, change in the amount of the surface peroxide species here is very limited. Approximately,

$$\frac{r}{r_0} = \left(\frac{[L_{ads}]}{[L_{ads}]_0}\right)^n \quad (5)$$

$$\ln r = \ln\left(\frac{\Delta C}{t}\right) = n\ \ln[L_{ads}] + |b \quad (b = \ln r_0 - n\ln[L_{ads}]_0 \text{ is a constant}) \quad (6)$$

$$\ln(\Delta C) = n\ \ln[L_{ads}] + b + \ln t \quad (7)$$

Fig. 5 presents the adsorption and degradation reaction in $CeO_2/H_2O_2$ system with various concentrations of AO7. The amount of adsorbed AO7, $[L_{ads}]$, can be estimated from Fig. 5, in which $[L_{ads}]$s are 8.1 mg/L, 10.4 mg/L, 11.2 mg/L and 12.4 mg/L, respectively. Accordingly, the value of $n$ (the apparent orders of reaction towards $L_{ads}$) can be obtained by identifying the quantitative relationship between AO7 concentration decrement in a fixed reaction time and $[L_{ads}]$ (Fig. 6). As a result, the value of $n$ is about $2.40 \pm 0.05$ calculated from the slopes of the fitting lines in Fig. 6. The fact that the $k$ value has a $(2.40 - 1.0) = 1.40$ apparent orders of reaction towards $L_{ads}$ confirms that increasing the initial concentration of AO7 not only increases the surface-adsorbed AO7 according to the Langmuir adsorption (Eq. (4)), but also increases the $k$ value by enhancing the activity of the reactive species (or sites) by complexing (and oxidation) with $H_2O_2$ at the surface of $CeO_2$. In other words, the quantitative analysis of the degradation kinetics of AO7 with various concentrations suggests again the important role the adsorbed AO7 plays in the release of surface $Ce^{3+}$ species from the complexes they formed with $H_2O_2$ via an adsorption-depend interfacial reaction.

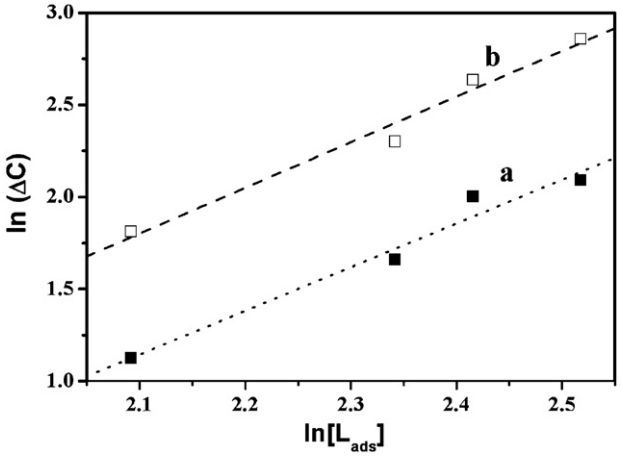


**Fig. 6.** AO7 concentration decrement ($\Delta C$) in the first (a) 1 h and (b) 2 h vs adsorbed amount of AO7 ($[L_{ads}]$) on the surface of $CeO_2$.

### 3.3. Degradation reaction kinetics evolution in the pre-mixed mode

In the absence of organic substances, the passivation of $CeO_2$ occurs because of the oxidation of $Ce^{3+}$ by $H_2O_2$ (Fig. 4b). Although the oxidation of $Ce^{3+}$ with $H_2O_2$ is ubiquitous here, one may notice that the degradation of AO7 carried out smoothly in the pre-adsorbed mode (Fig. 4a). Hence, we may come to an understanding that adsorption of AO7 can eliminate the passivation of $H_2O_2$ to the $CeO_2$.

Fig. 7 shows the degradation of AO7 with different concentration of $H_2O_2$ in the pre-mixed mode. The catalytic activity of $CeO_2$ can be gradually recovered by prolonging the reaction time, which greatly depends on the concentration of $H_2O_2$. The catalytic activity of $CeO_2$ is obviously recovered after 6 h and 12 h for 10 mM and 20 mM $H_2O_2$; however, in the presence of 80 mM $H_2O_2$, only a slight acceleration can be observed after a long time of 54 h. In the presence of high concentration of $H_2O_2$, the surface $Ce^{3+}$ sites of

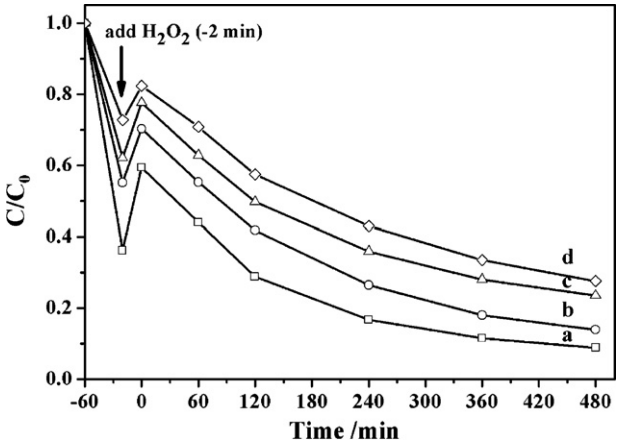


**Fig. 5.** Adsorption and degradation of AO7 in $CeO_2/H_2O_2$ system with (a) 20 mg/L, (b) 35 mg/L, (c) 50 mg/L, and (d) 70 mg/L of AO7. $[CeO_2] = 0.5$ g/L, $[H_2O_2] = 10$ mM.

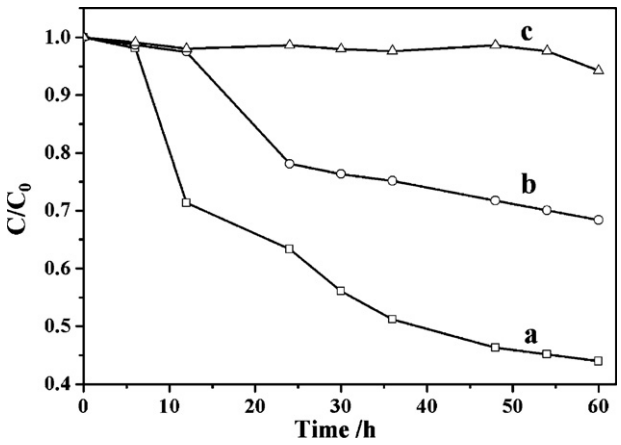


**Fig. 7.** Degradation of AO7 (pre-mixed mode) in $CeO_2/H_2O_2$ system with (a) 10 mM, (b) 20 mM, and (c) 80 mM $H_2O_2$. $[CeO_2] = 0.5$ g/L, $[AO7] = 35$ mg/L.

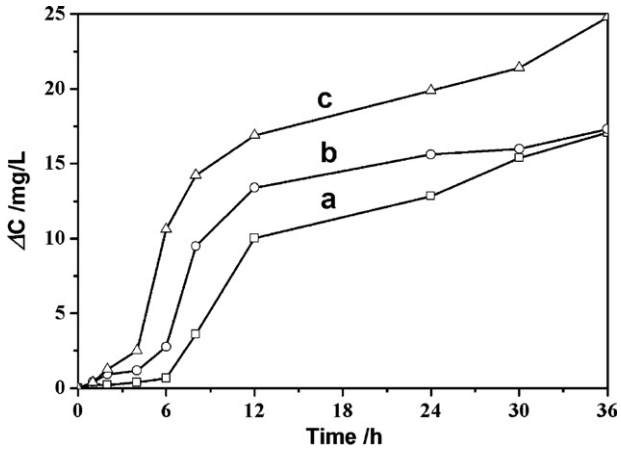


**Fig. 8.** Concentration decrement of AO7 (pre-mixed mode) in $CeO_2/H_2O_2$ system with (a) 35 mg/L, (b) 50 mg/L, and (c) 70 mg/L AO7. [$CeO_2$] = 0.5 g/L, [$H_2O_2$] = 10 mM.

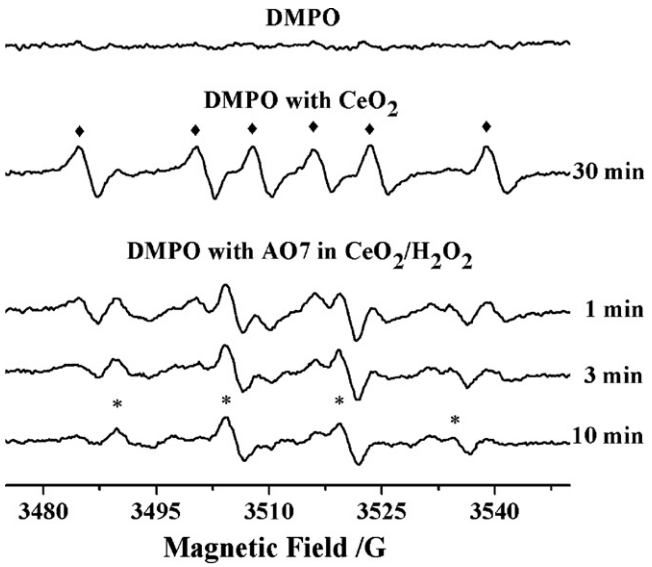


**Fig. 9.** DMPO spin trapping EPR spectra of (a) DMPO only, (b) DMPO and $CeO_2$ for 30 min, and DMPO with AO7 in $CeO_2/H_2O_2$ system for (c) 1 min, (d) 3 min, and (e) 10 min. (♦) DMPO-CCR; *: DMPO-•OH.

$CeO_2$ were solely complexed with $H_2O_2$ and transformed into surface peroxides species. The reactivity of surface peroxides species alone is very limited, and hence only a very slow AO7 concentration decrement can be observed at the initial stage. Along with the reaction, some $Ce^{3+}$ sites slowly began to be released from the reacted surface peroxides species. The released $Ce^{3+}$ sites, according to our previous work [25], can activate the reactivity of neighboring surface peroxides species, thus accelerating the degradation of AO7. As a result, the catalytic activity recovery of $CeO_2$ can be achieved after a reasonable interfacial reaction of AO7 with surface peroxides species. However, $H_2O_2$ of high concentration would complex immediately with the surface $Ce^{3+}$ sites just after the release, which is absolutely adverse to the catalytic activity recovery of $CeO_2$.

Such a proposal can be further confirmed from the AO7 degradation kinetics with $CeO_2/H_2O_2$ system (Fig. 8, in pre-mixed mode) for different concentration of AO7. As shown in Fig. 8, a significant AO7 degradation acceleration, that is the catalytic activity recovery of $CeO_2$, appears at about 6 h, 5 h and 4 h for 35 mg/L, 50 mg/L and 70 mg/L AO7, respectively. Increasing the concentration of AO7 accelerates the recovery of $CeO_2$ and enhances the reactivity of $CeO_2/H_2O_2$ system. A higher concentration of AO7 can improve the adsorption of AO7 at the surface of $CeO_2$, which benefits the protection of released $Ce^{3+}$ from over-complexing with of $H_2O_2$. Consequently the released $Ce^{3+}$ activates the reactivity of the neighboring surface peroxides species, and thus promotes the degradation of AO7 and further the release of $Ce^{3+}$ sites.

### 3.4. DMPO spin trapping EPR spectroscopy observation

DMPO spin trapping EPR spectroscopy measurement (Fig. 9) was carried out to study the possible active oxygen species formed in the reactions. The EPR spectrum of the $CeO_2$ alone with DMPO presents a typical sextet. According to the literatures [27], the sextet marked with "♦" is ascribed to the formation of DMPO-CCR (CCR, carbon-centered radical), which was stable and kept unchanged even after 30 min at ambient or several weeks at −15 °C in our lab. The interaction between DMPO and some transitional metal ions, such as manganese ion and cerium ion, results in a metal-DMPO complex, which then induces a molecular rearrangement to produce EPR active species, DMPO-CCR [28].

In the presence of $H_2O_2$, a typical signal of the DMPO-•OH adducts (1:2:2:1 quartet) gradually appeared while that of the DMPO-CCR adducts slowly disappeared. DMPO-•OH adducts could be formed in two possible pathways, attack of active •OH radical on the DMPO or surface reaction of DMPO with the surface peroxide-like species [29]. The peroxides species formed at the surface of $CeO_2$ in the pre-mixed mode are relatively chemically stable without organic contaminants (the brown color from the surface peroxide species was found retained after one week in ambient). Also considering that the degradation of AO7 depends greatly on its adsorption, we conclude that the reaction is mostly carried out at the surface of $CeO_2$ following an intermolecular rearrangement mechanism between the surface peroxides species with DMPO (and AO7) [24], in which •OH adduction occurs for organics oxidation.

### 3.5. Catalytic oxidation mechanism in the $CeO_2/H_2O_2$ system

$H_2O_2$ prefers to complex with cerium ion on the surface of $CeO_2$ to form surface peroxide species in $CeO_2/H_2O_2$ system, which is relatively chemically stable for days in the absence of the organic contaminants. An intermolecular rearrangement driven by surface peroxide species can occur when organics adsorb on its neighboring sites, which induces the oxidation of the neighboring adsorbed organic compounds. In other words, it is an organic adsorption-triggered degradation process. The amount of adsorbed organics is thus of great importance for the catalytic oxidation reactivity of $CeO_2$. However, the adsorption capability of $CeO_2$ towards the organics is mutable and relies on the surface state of $CeO_2$ itself. For instance, the surface oxygen vacancy, that is surface $Ce^{3+}$ site, will be unable to adsorb AO7 if it has been chemically complexed with $H_2O_2$. In the pre-mixed mode, over-complexation of $CeO_2$ with $H_2O_2$ hinders the adsorption of AO7 (Fig. 4) and hence decreases degradation of AO7. Besides, $Ce^{3+}$ plays a key role in promoting the catalytic activity of $CeO_2$ [30]. Complexation of $CeO_2$ with $H_2O_2$ chemically changes the surface state of $CeO_2$ by transforming $Ce^{3+}$ site into surface peroxide species. Therefore, over-complexation with $H_2O_2$ significantly reduces the amount of surface $Ce^{3+}$ resulting in hindering catalytic oxidation reaction towards the AO7. On the other hand, the adsorption of organic contaminants occupies the oxygen vacancies ($Ce^{3+}$), as well as consumes the surface peroxide species to release $Ce^{3+}$, both of which protect the $Ce^{3+}$ against oxidation, and hence accelerate the catalytic oxidation reaction of AO7. As shown in Fig. 6, the degradation of AO7 presents an apparent order of 2.40 towards its adsorption amount $L_{ads}$ on $CeO_2$, which verifies the activation role of adsorbed AO7 on the release of $Ce^{3+}$ from the over-complexation with $H_2O_2$.

In the pre-adsorbed mode for the degradation of AO7 in $CeO_2/H_2O_2$ system, adsorption-desorption equilibrium of AO7 is initially established on the surface of $CeO_2$. The subsequent addition of $H_2O_2$ induces a competitive adsorption between $H_2O_2$ and AO7, which induce the partial desorption and a simultaneous degradation of adsorbed AO7. $H_2O_2$ with a higher concentration results in quicker desorption as well as larger degradation reaction constant ($k$) for AO7. However, it also leads to over-complexation $H_2O_2$ with $CeO_2$, which later hinders the further degradation of AO7 as shown in Fig. 2. On the other hand, when degradation of AO7 was carried out in the pre-mixed mode, the surface of $CeO_2$ was well complexed (and thus oxidized) with $H_2O_2$, hence, hindering adsorption of AO7 molecules with $H_2O_2$. In this case, the surface peroxide species shows little activity as almost all the surface $Ce^{3+}$ have been oxidized by $H_2O_2$, leading to limited amount of adsorbed AO7 which results in further deterioration in the degradation kinetics of AO7. Increasing the concentration level of $H_2O_2$ in pre-mixed mode prolongs the recovery of $CeO_2$ and induces much lower reactivity of $CeO_2/H_2O_2$ system (Fig. 7). Inversely, increasing the concentration of AO7 would help the competitive adsorption of AO7, which benefits the degradation of AO7. Meanwhile, the surface $Ce^{3+}$ is slowly released from the surface peroxide species, some of which would be occupied with AO7 which help them remain in un-oxidized state $Ce^{3+}$. As a result, the reactivity of the $CeO_2/H_2O_2$ system slowly recovers, and the higher the concentration of AO7, the quicker the recovery of the reactivity of the $CeO_2/H_2O_2$ system for the degradation of AO7 (Fig. 8).

## 4. Conclusions

Nano-$CeO_2$ with cubic lattice structure was prepared by the precipitation method. The adsorption, desorption and the degradation of AO7 were then investigated with $CeO_2$ in the presence of $H_2O_2$ in both pre-adsorbed mode and pre-mixed mode. The degradation of AO7 relies significantly on its adsorption on the surface of $CeO_2$. Experimentally, the degradation of AO7 presents an apparent order of 2.40 towards its adsorption amount on the surface of $CeO_2$. Increasing the concentration of $H_2O_2$ increases the degradation reaction rate constant of AO7 in a positive linear relationship at the initial stage, but later hinders the further degradation of AO7 due to the over-complexation of $Ce^{3+}$ with $H_2O_2$. The pre-mixed mode is unfavorable for AO7 degradation, as almost all of the surface $Ce^{3+}$ are pre-oxidized into surface peroxide species by $H_2O_2$ and thus be adverse for the AO7 adsorption as well as the activation of AO7 degradation. Fortunately, the reactivity of $CeO_2$ can slowly recover with increase in concentration of AO7, which competitively adsorbs on the $CeO_2$ and gradually initiates the release of the surface $Ce^{3+}$ by consuming the surface peroxide species. The higher the concentration of AO7 is, the quicker the recovery of the reactivity of the $CeO_2/H_2O_2$ system for the degradation of AO7. The AO7 degradation kinetics revealed in this work verifies again that the degradation of organics in $CeO_2/H_2O_2$ system is adsorption-triggered and carried out just on the surface of $CeO_2$ and the $Ce^{3+}$ in reduced state is very essential for activation of the catalytic oxidation activity of surface peroxide species. EPR studies show that the surface peroxide species oxidize the organics via hydroxyl adduct route.

## Acknowledgment

This work was supported by the National Nature Science Foundations of China (21177039) and the Fundamental Research Funds for the Central Universities.

## References

[1] S.I. Matsumoto, Catalysis Today 90 (2004) 183–190.
[2] F. Vindigni, M. Manzoli, A. Damin, T. Tabakova, A. Zecchina, Chemistry: A European Journal 17 (2011) 4356–4361.
[3] J.A. Rodriguez, S. Ma, P. Liu, J. Hrbek, J. Evans, M. Perez, Science 318 (2007) 1757–1760.
[4] C.T. Campbell, C.H.F. Peden, Science 309 (2005) 713–714.
[5] F. Esch, S. Fabris, L. Zhou, T. Montini, C. Africh, P. Fornasiero, G. Comelli, R. Rosei, Science 309 (2005) 752–755.
[6] Y.W. Zhang, R. Si, C.S. Liao, C.H. Yan, Journal of Physical Chemistry B 107 (2003) 10159–10167.
[7] S.D. Park, J.M. Vohs, R.J. Gorte, Nature 404 (2000) 265–267.
[8] C. Laberty-Robert, J.W. Long, K.A. Pettigrew, R.M. Stroud, D.R. Rolison, Advanced Materials 19 (2007) 1734–1739.
[9] T.H. Shin, S. Ida, T. Ishihara, Journal of the American Chemical Society (2011).
[10] J. Kašpar, P. Fornasiero, M. Graziani, Catalysis Today 50 (1999) 285–298.
[11] A. Trovarelli (Ed.), Catalysis by Ceria and Related Materials, Imperial College Press, London, 2002.
[12] A. Karakoti, S. Singh, J.M. Dowding, S. Seal, W.T. Self, Chemical Society Reviews 39 (2010) 4422.
[13] S. Singh, T. Dosani, A.S. Karakoti, A. Kumar, S. Seal, W.T. Self, Biomaterials 32 (2011) 6745–6753.
[14] T. Pirmohamed, J.M. Dowding, S. Singh, B. Wasserman, E. Heckert, A.S. Karakoti, J.E.S. King, S. Seal, W.T. Self, Chemical Communications 46 (2010) 2736.
[15] C. Korsvik, S. Patil, S. Seal, W.T. Self, Chemical Communications (2007) 1056.
[16] E.G. Heckert, A.S. Karakoti, S. Seal, W.T. Self, Biomaterials 29 (2008) 2705–2709.
[17] E.G. Heckert, S. Seal, W.T. Self, Environmental Science & Technology 42 (2008) 5014–5019.
[18] M. Das, S. Patil, N. Bhargava, J.-F. Kang, L.M. Riedel, S. Seal, J.J. Hickman, Biomaterials 28 (2007) 1918–1925.
[19] E.-J. Park, J. Choi, Y.-K. Park, K. Park, Toxicology 245 (2008) 90–100.
[20] Y. Xue, Q.F. Luan, D. Yang, X. Yao, K.B. Zhou, Journal of Physical Chemistry C 115 (2011) 4433–4438.
[21] P. Massa, F. Ivorra, P. Haure, R. Fenoglio, The Journal of Hazardous Materials 190 (2011) 1068–1073.
[22] S.S. Lin, C.L. Chen, D.J. Chang, C.C. Chen, Water Research 36 (2002) 3009–3014.
[23] A.F. Rossi, N. Amaral-Silva, R.C. Martins, R.M. Quinta-Ferreira, Applied Catalysis B: Environmental (2011), http://dx.doi.org/10.1016/j.apcatb.2011.10.006.
[24] W.D. Cai, F. Chen, X.X. Shen, L.J. Chen, J.L. Zhang, Applied Catalysis B: Environmental 101 (2010) 160–168.
[25] P.F. Ji, L.Z. Wang, F. Chen, J.L. Zhang, Chemcatchem 2 (2010) 1552–1554.
[26] P.F. Ji, J.L. Zhang, F. Chen, M. Anpo, Applied Catalysis B: Environmental 85 (2009) 148–154.
[27] M. Danilczuk, A.J. Perkowski, S. Schlick, Macromolecules 43 (2010) 3352–3358.
[28] F.A. Villamena, D.R. Crist, Journal of the Chemical Society, Dalton Transactions 23 (1998) 4055–4062.
[29] P.M. Hanna, W. Chamulitrat, R.P. Mason, Archives of Biochemistry and Biophysics 296 (1992) 640–644.
[30] X.W. Liu, K.B. Zhou, L. Wang, B.Y. Wang, Y.D. Li, Journal of the American Chemical Society 131 (2009) 3140–3141.